NAVAL SHIP RESEARCH AND DEVELOPMENT CENTER
Bethesda, Md. 20034

EVALUATION OF A ROTATING DISK APPARATUS: DRAG OF A DISK ROTATING IN A VISCOUS FLUID

by

John J. Nelka

APPROVED FOR PUBLIC RELEASE: DISTRIBUTION UNLIMITED

SHIP PERFORMANCE DEPARTMENT
RESEARCH AND DEVELOPMENT REPORT

July 1973 Report 3851

The Naval Ship Research and Development Center is a U. S. Navy center for laboratory effort directed at achieving improved sea and air vehicles. It was formed in March 1967 by merging the David Taylor Model Basin at Carderock, Maryland with the Marine Engineering Laboratory at Annapolis, Maryland.

Naval Ship Research and Development Center

Bethesda, Md. 20034

MAJOR NSRDC ORGANIZATIONAL COMPONENTS

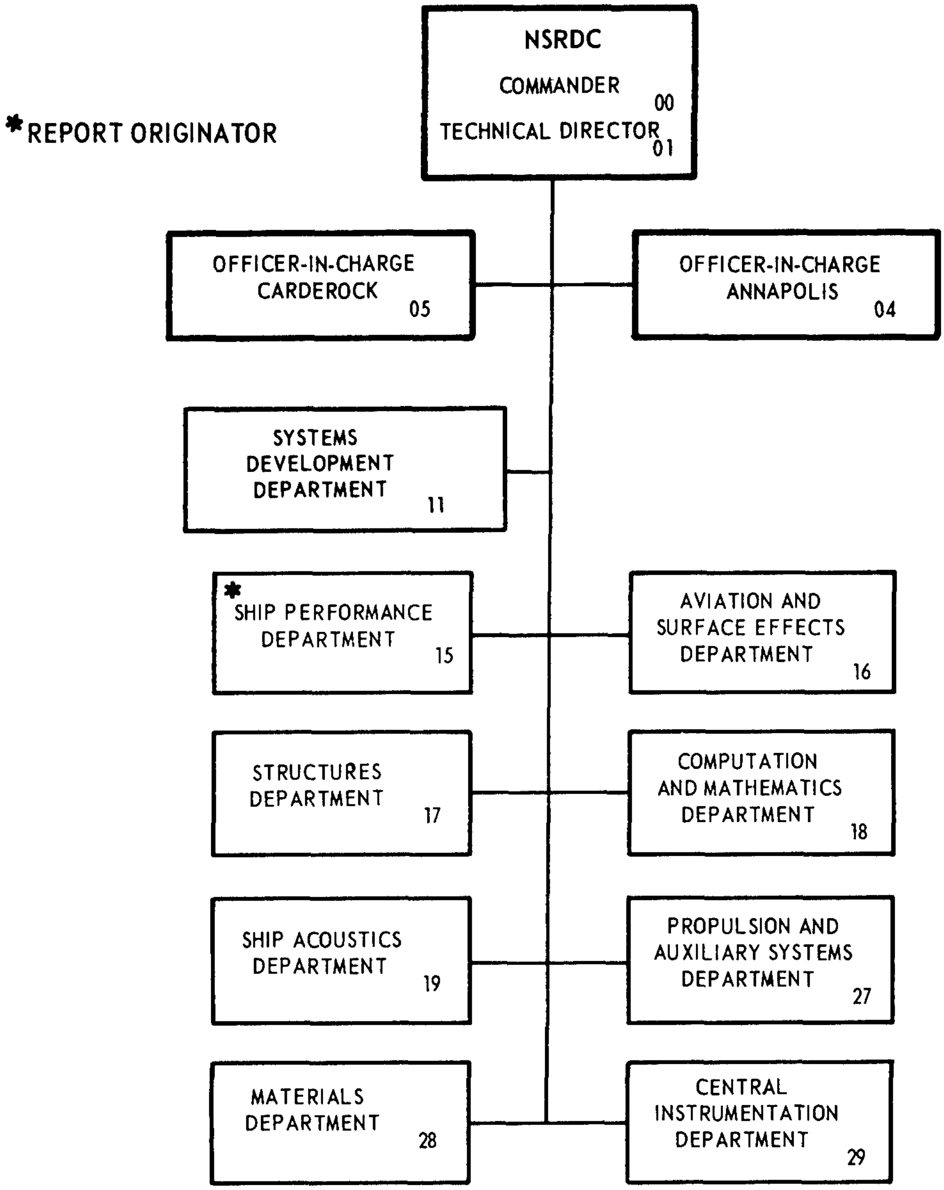

NDW-NSRDC 3960/43b (Rev. 3-72)

GPO 928-108

DEPARTMENT OF THE NAVY
NAVAL SHIP RESEARCH AND DEVELOPMENT CENTER
Bethesda, Md. 20034

EVALUATION OF A ROTATING DISK APPARATUS:
DRAG OF A DISK ROTATING IN A VISCOUS FLUID

by

John J. Nelka

July 1973 Report 3851

TABLE OF CONTENTS

LIST OF FIGURES

LIST OF TABLES

NOTATION

A,B	Constants in the Goldstein velocity profiles; A = 2.5; B = 5.5
b	Thickness of disk
C_m	Moment Coefficient, $C_m = 2M/\frac{1}{2}\rho\,\omega^2 R^5$
C'_m	Moment coefficient due to disk and its edge
C_τ	Shear coefficient
F_{av}	Average shear force acting on one side of disk
$F_{r,\phi,z}$	Body forces in radial, tangential, and axial directions
F,G,H	Nondimensional velocity profiles in r,ϕ, and z directions
k_s	Characteristic roughness height
M	Moment due to one side of disk
p	Pressure
R	Radius of disk
R_n	Reynolds number, $R_n = \omega R^2/\nu$
r	Radial direction or radius
t	Time
U_∞	Free-stream velocity
u,v,w	Velocity in radial, tangential, and axial directions
v*	Friction velocity of $v^* = \sqrt{\tau_o/\rho}$
z	Axial direction
δ	Boundary layer thickness
ζ	Nondimensional axial distance from disk surface
ζ_o	Nondimensional boundary layer thickness
η	Axial distance from disk surface
μ	Coefficient of dynamic viscosity of fluid

ν	Coefficient of kinematic viscosity, $\nu = \mu/\rho$
ρ	Density of fluid
τ_{av}	Average shear acting on one side of disk
$\tau_{r,\phi}$	Shear in radial and tangential directions
τ_{SHIP}	Shear stress acting on ship hull
α	Ratio of τ_r/τ_ϕ
ϕ	Tangential direction
ω	Angular velocity

ABSTRACT

A rotating disk apparatus, designed to attain high shear stresses comparable to those about hulls of full-scale ships is evaluated. It was thought that this apparatus could provide a convenient and inexpensive method to study frictional resistance of a full-scale ship. For a full-scale ship Reynolds number of 10^9, the average shear coefficient is approximately 0.0015. To attain the shear stress associated with such a shear coefficient, the angular velocity for a 2-ft diam disk is required to be about 350 rpm in water or about 10,000 rpm in air. These angular velocities were not obtainable with the disk apparatus described. However, the investigation did provide worthwhile results for lower shear stress values. Shear stresses were not measured but were inferred from measurements of disk moments. Two disk surfaces are evaluated, hydraulically smooth and sandpaper rough. For the smooth and rough surface disks in air, the experimental moment coefficients are generally greater than the theoretical predictions. Only the smooth surface disk was evaluated in water with results lower than predictions. The maximum Reynolds numbers attained in air and in water were 1.34×10^6 and 1.55×10^6, respectively.

ADMINISTRATIVE INFORMATION

This work was authorized under the General Hydromechanics Research Program of the Naval Ship Research and Development Center. Funding was provided by Naval Ship Systems Command, Subproject S-R009 01 01, Task 0104, Work Unit 1-1589-086.

INTRODUCTION

High shear stresses, comparable to those for hulls of full-scale ships are difficult to achieve in the laboratory. One possible way to overcome this difficulty is through the use of a disk rotating at high speed. Thus, if successful, a rotating-disk apparatus could provide a convenient and inexpensive way to analyze ship-size, added frictional resistance due to roughness. A more accurate evaluation of added frictional resistance would help to determine how to improve the speed and power characteristics of ships. A rotating-disk apparatus has been developed and evaluated using a 2-ft diam disk.

COMPARISON OF DISK AND FULL-SCALE SHEAR STRESSES

The angular velocity of a disk, required to yield the same average shear stress on the disk as that of the full-scale ship hull, is now determined. For the rotating disk, to obtain the order of magnitude of the circumferential or disk shear, it is assumed that the shear acting on the disk from 50- to 100-percent radius contributes all of the moment. Therefore, for an average moment arm r_{av} of 0.75 R, where R is disk radius and an area over which the shear acts of $0.75\pi R^2$, the moment due to one side of the disk is

$$M = F_{av} \times r_{av}$$

where $F_{av} \equiv$ average shear times the area = $(\tau_{av})_c\ 0.75\pi R^2$, and $(\tau_{av})_c$ = average circumferential shear.

Therefore

$$M = (0.75)^2 \pi R^3 (\tau_{av})_c$$

or

$$(\tau_{av})_c = \frac{M}{(0.75)^2 \pi R^3}$$

For shear stress of the full-scale ship, the average skin-friction coefficient as obtained from flat plate theory[1] is

$$(C_\tau)_{ship} = \frac{\tau_{ship}}{\frac{1}{2}\rho_s U_\infty^2} = 0.0015$$

at a Reynolds number (R_n) of 10^9 or

$$\tau_{ship} = \frac{1}{2}\rho_s\, U_\infty^2\, (C_\tau)_{ship}$$

where τ_{ship} is the shear acting on the ship hull
ρ_s is density of fluid in which the ship is immersed
U_∞ is the velocity of the ship

[1]Schlichting, H., "Three-Dimensional Boundary Layer Flow," Deutsche Forschungsanstalt Fur Luftfahrt E.V., Institut Fur Aerodynamik Report 61/3a, pp 9-10 (Sep 1961).

For $(\tau_{av})_c = \tau_{ship}$

$$\frac{M}{(0.75)^2 \pi R^3} = \frac{1}{2} \rho_s U_\infty^2 (C_\tau)_{ship}$$

Defining C_m so that $M = \frac{1}{2} C_m (1/2 \rho_D \omega^2 R^5)$ where ρ_D is the density of fluid in which the disk is rotating, and ω is the disk angular velocity. Then

$$\frac{\frac{1}{4} C_m \rho_D \omega^2 R^5}{(0.75)^2 \pi R^3} = \frac{1}{2} \rho_s U_\infty^2 (C_\tau)_{ship}$$

Solving for ω yields

$$\omega = 1.88 \left[\frac{\rho_s}{\rho_D}\right]^{1/2} \left[\frac{C_\tau}{C_m}\right]^{1/2} \frac{U_\infty}{R} \text{ rad/sec}$$

or

$$\omega = 17.95 \left[\frac{\rho_s}{\rho_D}\right]^{1/2} \left[\frac{C_\tau}{C_m}\right]^{1/2} \frac{U_\infty}{R} \text{ rpm}$$

For the disk rotating in water, $\rho_s = \rho_D$ and for $U_\infty = 20$ knots, $R = 1$ ft, $R_n = 10^9$ with $C_\tau = 0.0015$, $C_m{}^* \approx 4.5 \times 10^{-3}$, for $R_n = 10^9$, the angular velocity required to attain ship-size frictional resistance is approximately 350 rpm. For the disk in air, the angular velocity required is 10,000 rpm.

The low angular velocity of 350 rpm was not attainable with the present apparatus because of increased water surface movement. The high angular velocity of 10,000 rpm was not attainable because of undesirable disk-apparatus vibration.

If the disk radius were increased to 2 ft and rotated in water, the ship-size shear stresses could be attained.

DESCRIPTION OF BOUNDARY LAYER

The flow of a viscous fluid over a surface is characterized by a friction layer or boundary layer of finite thickness in the vicinity of the surface. For viscous flow over a semi-infinite flat plate, the boundary

---

*Extrapolated from data of Figure 1.

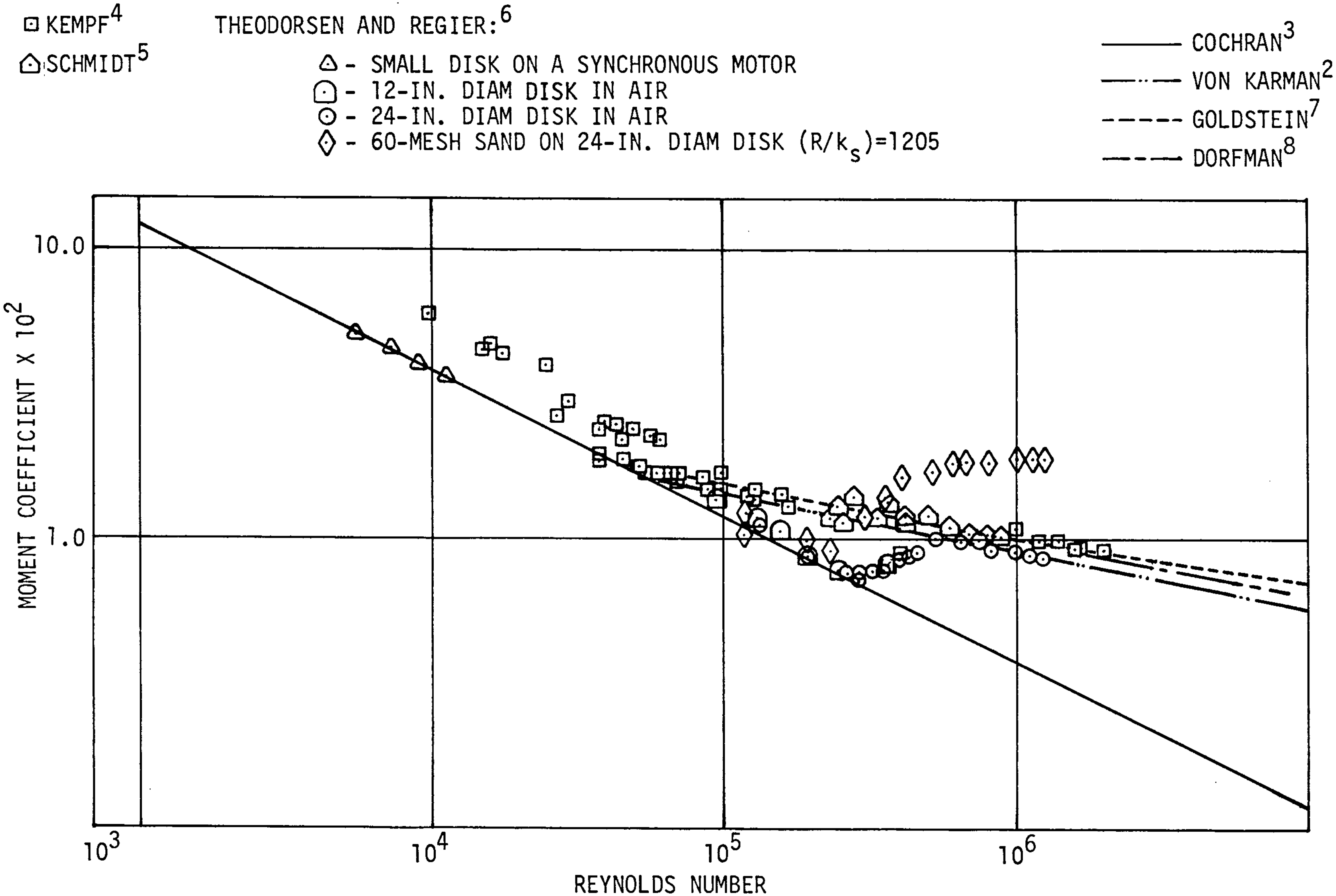

Figure 1 - Previous Results of the Moment Coefficient as a Function of Reynolds Number for a Disk Rotating in a Viscous Fluid Initially at Rest

layer is two dimensional as shown in Figure 2, while for the flow due to a disk rotating in a fluid initially at rest, the boundary layer is three dimensional as shown in Figure 3. The velocity of the fluid satisfies the no-slip condition at the surface and then either increases in the case of the flat plate or decreases in the case of the rotating disk to the free-stream velocity, which is zero for the rotating disk. For the flat plate and disk, the normal distance from the surface where the velocity is 99 percent of the free-stream velocity and 1 percent of the disk velocity, respectively, is termed "boundary layer thickness δ." For small or negligible velocity fluctuations within the boundary layer, the boundary layer is termed "laminar"; as the velocity fluctuations increase, the boundary layer is termed "transitional"; and for large velocity fluctuations, the boundary layer is termed "turbulent." The intensity of these velocity fluctuations is primarily a function of the free-stream velocity, the surface roughness, and the distance from the initial formation of the boundary layer.

FLOW DUE TO A ROTATING DISK

The fluid surrounding the rotating disk is initially at rest. As the disk begins to rotate, the fluid near the surface of the disk is strongly affected by the friction between the fluid layer, which adheres to the disk surface, and the layers of fluid which make up the boundary layer. If it is assumed that the only pressure change is in the direction normal to the disk surface, there is an imbalance between the friction and the centrifugal forces in the radial direction, the centrifugal force being dominant. This causes the fluid to be forced outward. An axial flow toward the disk compensates for the outward flow of fluid.

DISK-FORCE BALANCE

To understand what forces contribute to the moment on a disk rotating in a viscous fluid, a disk force balance is undertaken.

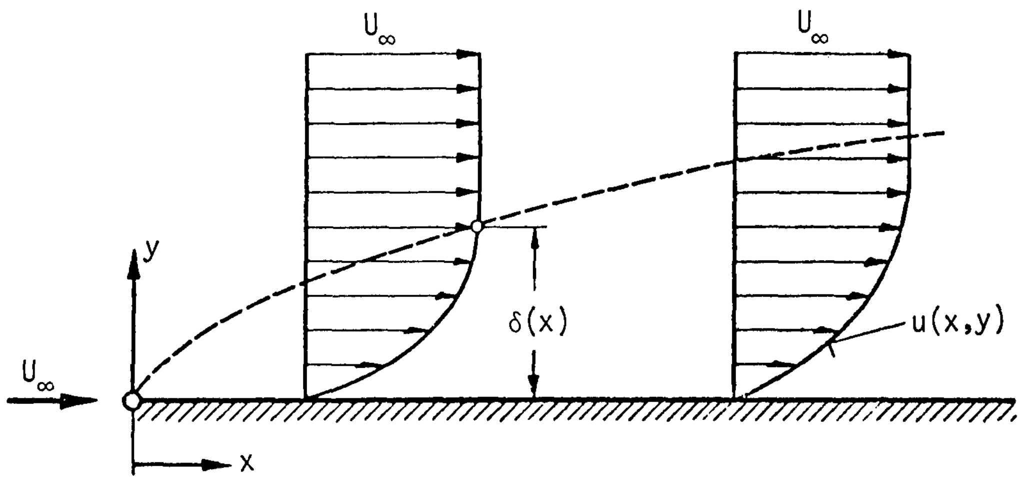

Figure 2 - Boundary Layer on a Flat Plate

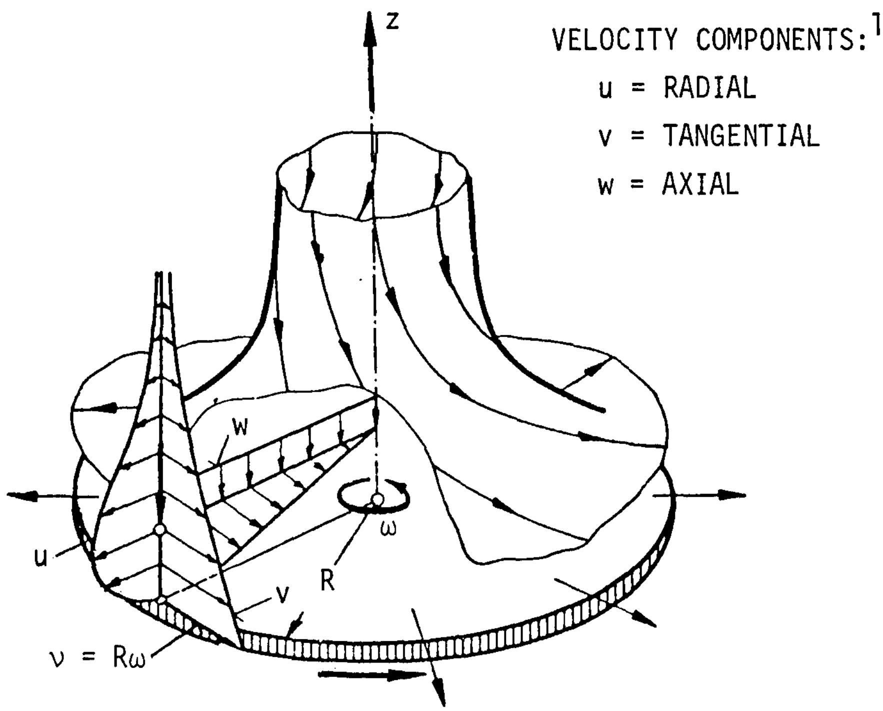

Figure 3 - Boundary Layer Flow on a Disk Rotating in a Fluid Initially at Rest

Equations (1a) and (1b), Reference 2, are the steady-state momentum equations in the radial and circumferential directions for a differential fluid element of thickness δ as derived in Appendix A. Higher order differentials have been neglected, and $p = p(z)$ has been assumed.

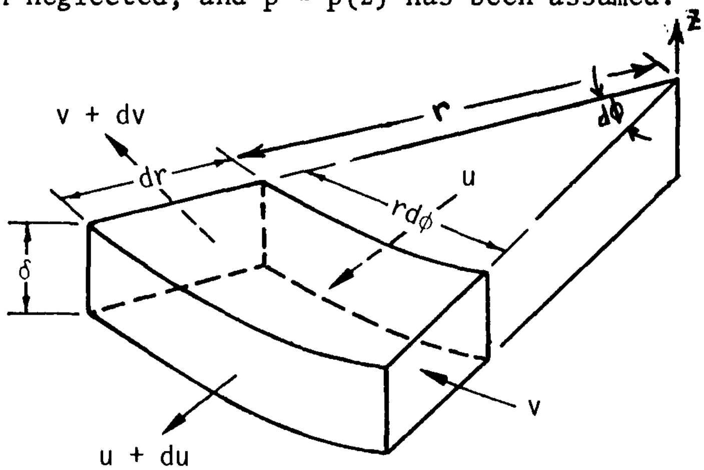

Fluid Element of Thickness δ

where r is radius

u,v are velocities in radial and tangential direction

z is axial direction

δ is boundary layer thickness

ϕ is tangential direction

Radial Direction

$$\frac{d}{dr}\left(2\pi r\rho \int_0^\delta u^2\, dz\right) dr - 2\pi r\rho \left[\int_0^\delta \frac{v^2}{r}\, dz\right] dr = - 2\pi r \quad \tau_r \, dr \qquad (1a)$$

Momentum Change — Centrifugal Force — Radial Shear Force

where ρ is density of fluid, and τ_r is shear in radial direction.

---

[2] von Karman, T., "On Laminar and Turbulent Friction," National Advisory Committee for Aeronautics TM 1092, Vol I, No. 4, pp 20-30 (Aug 1921).

Circumferential Direction

$$\frac{d}{dr}\left(2\pi r^2 \rho \int_0^\delta uv\, dz\right) dr = -\, 2\pi r^2\, \tau_\phi\, dr = -\, dM \qquad (1b)$$

Angular Momentum — Moment Due to Circumferential Shear Force

where M is moment due to one side of disk, and τ_ϕ is shear in circumferential direction. Integration of Equation (1b) yields the moment due to a finite disk, if the disk edge effects are neglected.

It is seen from Equation (1b) that the resisting torque of a disk rotating in a fluid which is initially at rest is a measure of the circumferential shear forces acting on the disk surface and can be calculated if the radial and tangential velocities are known throughout the whole boundary layer.

NAVIER-STOKES EQUATIONS, CONTINUITY EQUATION

By applying the boundary conditions for a flow about a rotating disk to the Navier-Stokes equations, and the continuity equation the tangential and radial velocity profiles can be found for a laminar boundary layer. The boundary conditions for a disk rotating at ω in a fluid initially at rest are

$$\text{at } z = 0:\ u = 0,\ v = r\omega,\ w = 0$$

$$\text{at } z = \delta:\ u \approx 0,\ v \approx 0$$

(2)

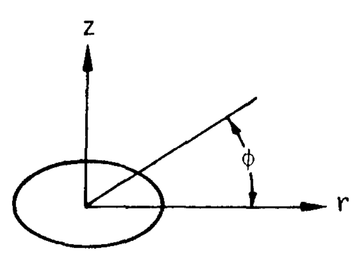

Coordinate system fixed in space with its origin at center of disk.

The Navier-Stokes equations in cylindrical coordinates are

$$\rho\left(\frac{\partial u}{\partial t}+u\frac{\partial u}{\partial r}+\frac{v}{r}\frac{\partial u}{\partial \phi}-\frac{v^2}{r}+w\frac{\partial u}{\partial z}\right)=F_r-\frac{\partial p}{\partial r}+\mu\left(\frac{\partial^2 u}{\partial r^2}+\frac{1}{r}\frac{\partial u}{\partial r}-\frac{u}{r^2}\right.$$

$$\left.+\frac{1}{r^2}\frac{\partial^2}{\partial \phi}\left(\frac{u}{2}\right)-\frac{2}{r^2}\frac{\partial v}{\partial \phi}+\frac{\partial^2 u}{\partial z^2}\right)$$

$$\rho\left(\frac{\partial v}{\partial t}+u\frac{\partial v}{\partial r}+\frac{v}{r}\frac{\partial v}{\partial \phi}+\frac{uv}{r}+w\frac{\partial v}{\partial z}\right)=F_\phi-\frac{1}{r}\frac{\partial p}{\partial \phi}+\mu\left(\frac{\partial^2 v}{\partial r^2}+\frac{1}{r}\frac{\partial v}{\partial r}\right. \qquad (3)$$

$$\left.-\frac{v}{r^2}+\frac{1}{r^2}\frac{\partial^2 v}{\partial \phi^2}+\frac{2}{r^2}\frac{\partial u}{\partial \phi}+\frac{\partial^2 v}{\partial z^2}\right)$$

$$\rho\left(\frac{\partial w}{\partial t}+u\frac{\partial w}{\partial r}+\frac{v}{r}\frac{\partial w}{\partial \phi}+w\frac{\partial w}{\partial z}\right)=F_z-\frac{\partial p}{\partial z}+\mu\left(\frac{\partial^2 w}{\partial r^2}+\frac{1}{r}\frac{\partial w}{\partial r}+\frac{1}{r^2}\frac{\partial^2 w}{\partial \phi^2}+\frac{\partial^2 w}{\partial z^2}\right)$$

where t is time

w is velocity in axial direction

F_r is body force in radial direction

F_ϕ is body force in ϕ-direction

F_z is body force in z-direction

p is pressure

μ is coefficient of dynamic viscosity

The continuity equation in cylindrical coordinates is:

$$\frac{\partial u}{\partial r}+\frac{u}{r}+\frac{1}{r}\frac{\partial v}{\partial \phi}+\frac{\partial w}{\partial z}=0 \qquad (4)$$

Applying the boundary conditions of Equation (2) to Equations (3) and (4); assuming steady-state, rotational symmetry ($\partial/\partial\phi = 0$); and neglecting the body forces yields

$$u\frac{\partial u}{\partial r}-\frac{v^2}{r}+w\frac{\partial u}{\partial z}=-\frac{1}{\rho}\frac{\partial p}{\partial r}+\nu\left(\frac{\partial^2 u}{\partial r^2}+\frac{\partial}{\partial r}\left(\frac{u}{r}\right)+\frac{\partial^2 u}{\partial z^2}\right)$$

$$u\frac{\partial v}{\partial r}+\frac{uv}{r}+w\frac{\partial v}{\partial z}=\nu\left(\frac{\partial^2 v}{\partial r^2}+\frac{\partial}{\partial r}\left(\frac{v}{r}\right)+\frac{\partial^2 v}{\partial z^2}\right)$$

$$u \frac{\partial w}{\partial r} + w \frac{\partial w}{\partial z} = -\frac{1}{\rho}\frac{\partial p}{\partial z} + \nu \left(\frac{\partial^2 w}{\partial r^2} + \frac{1}{r}\frac{\partial w}{\partial r} + \frac{\partial^2 w}{\partial z^2}\right) \tag{5}$$

$$\frac{\partial u}{\partial r} + \frac{u}{r} + \frac{\partial w}{\partial z} = 0$$

where ν is the coefficient of kinematic viscosity. From Reference 1, Equation (5) yields velocity profiles of the form

$$\begin{aligned} u &= r\omega\, F(\zeta) \\ v &= r\omega\, G(\zeta) \\ w &= \sqrt{\nu\omega}\, H\ (\zeta) \\ p &= p(z) = \rho\nu\omega\, p(\zeta) \text{ where } \zeta = z\sqrt{\omega/\nu} \end{aligned} \tag{6}$$

where F, G, and H are the nondimensional velocities in the r, ϕ, z directions, functions only of ζ to be determined.

Inserting Equation (6) into Equation (5) yields

$$\begin{aligned} &2F + H' = 0 \\ &F^2 + F'H - G^2 - F'' = 0 \\ &2FG + HG' - G'' = 0 \\ &p' + HH' - H'' = 0 \end{aligned} \tag{7}$$

where ' denotes derivative with respect to ζ.

The appropriate boundary conditions are

$$\begin{aligned} &\text{at } \zeta = 0: \quad F = 0, \quad G = 1, \quad H = 0, \quad p = 0 \\ &\text{at } \zeta = \infty: \quad F = 0, \quad G = 0 \end{aligned} \tag{8}$$

The solution of Equations (7) by von Karman[2] and Cochran[3] will be discussed in the next section.

The moment coefficient, C_m, is defined as

$$C_m = \frac{2M}{1/2\ \rho\omega^2\ R^5}$$

where M is the moment due to one side of the disk, and R is the disk radius.

---

[3]Cochran, W.G., "The Flow Due to a Rotating Disc," Proceedings of the Cambridge Philosophical Society, Vol. 30, pp. 365-375 (1934).

The Reynolds number R_n is defined as

$$R_n = \frac{\omega R^2}{\nu}$$

PREVIOUS INVESTIGATIONS

THEORETICAL

Von Karman[2] analyzed the laminar and turbulent flow about a disk rotating in a fluid initially at rest. For the laminar case he solved Equation (7), using the boundary conditions of Equation (8) and approximating F and G by

$$F = a\frac{\zeta}{\zeta_o}\left(1 - \frac{\zeta}{\zeta_o}\right)^2\left(1 + \frac{2\zeta}{\zeta_o}\right) - \frac{1}{2}\left(\frac{\zeta}{\zeta_o}\right)^2\left(1 - \frac{\zeta}{\zeta_o}\right)^2$$

$$G = \frac{1}{2}\left(2 + \frac{\zeta}{\zeta_o}\right)\left(1 - \frac{\zeta}{\zeta_o}\right)^2$$

where a is a constant and ζ_o is the nondimensional boundary layer thickness. Velocity profiles F and G are nondimensional power series in ζ/ζ_o, which satisfy boundary conditions of Equation (8).

Von Karman also assumed that $F = dF/d\zeta = 0$ and $G = dG/d\zeta = 0$ at $\zeta = \zeta_o$. Upon integrating Equation (7), von Karman found

$$a = 1.026$$

$$\zeta_o = 2.58$$

With F, and G and Equation (1b), the moment for both sides of the disk, neglecting edge effects, is: $2M = 1.84\ R^4\ \rho\nu^{1/2}\ \omega^{3/2}$, which yields a moment coefficient $C_m = 3.68/[R_n]^{1/2}$. For the turbulent case, von Karman used Equation (1b) and assumed velocity profiles for boundary layers found in pipes of the form

$$u = \alpha r\omega(z/\delta)^{1/7}\cdot[1 - z/\delta]$$

$$v = r\omega\ [1 - (z/\delta)^{1/7}]$$

where α is equal to τ_r/τ_ϕ

z is the axial distance from disk surface

δ is the boundary layer thickness r is the radius

ω is the angular velocity

Equations (1a) and (1b) are satisfied when

$$\alpha = \tau_r/\tau_\phi = 0.162$$

$$\delta = \beta r^{3/5} \text{ where } \beta = 0.522\ (\nu/\omega)^{1/5}$$

The moment for both sides of the disk for the turbulent case is: $2M = 0.0728\ R^5\omega^2\rho(\nu/R^2\omega)^{1/5}$, which yields a moment coefficient $C_m = 0.146/R_n^{1/5}$. Figure 3 shows a comparison between the theoretical results of von Karman for the turbulent boundary layer and experimental data of Kempf,[4] Schmidt,[5] and Theodorsen and Regier.[6]

Cochran[3] analyzed the laminar flow about a disk rotating in a fluid initially at rest. The Cochran solution was obtained by using a power series near $\zeta = 0$ and an asymptotic series for large values of ζ and then matching their solutions at some intermediate values of ζ. Cochran found the moment for both sides of the disk, neglecting edge effects, to be

$$2M = (0.616)\pi\rho R^4\ \nu^{1/2}\ \omega^{3/2}$$

giving a moment coefficient $C_m = 3.87/R_n^{1/2}$. Cochran found an error in the von Karman integration. The Cochran correction of the von Karman solution yielded $2M = 1.69\ \rho R^4\ \nu^{1/2}\ \omega^{3/2}$, resulting in a moment coefficient $C_m = 3.38/(R_n)^{1/2}$. The Cochran theoretical result is presented in Figure 3.

---

[4]Kempf, G., "Uber Reibungswiderstand Rotierender Scheiben," Vortrage auf dem Gebiet der Hydro- und Aerodynamik, Innsbruck Congress (1922); Berlin, 168 (1924).

[5]Schmidt, W., "Ein einfaches Meßverfahren fur Drehmoments," Z. VDI. 65, pp. 441-444 (1921).

[6]Theodorsen, T. and R. Regier, "Experiments on Drag of Revolving Disks, Cylinders, and Streamline Rods at High Speeds," National Advisory Council for Aeronautics Report 793, pp. 4-6 (1945).

Goldstein[7] discussed the turbulent boundary layer on a rotating disk. He assumed a logarithmic velocity profile since the one-seventh-power law would be valid for values of $v^*\eta/\nu \leq 600$. This profile led to a better curve fit of the moment data of Kempf[4] and Schmidt[5]. The logarithmic profile obtained by Goldstein is

$$\bar{U} = Av^* \log (v^*\eta/\nu) + B \text{ for } v^*\eta/\nu > 30$$

where A and B are constants,

v^* is the friction velocity,

η is the axial distance from disk surface,

ν is the kinematic viscosity, and

$\bar{U} = \sqrt{u^2 - (v-r\omega)^2}$

Goldstein obtained a moment coefficient of the form

$$C_m^{-1/2} = 1.97 \log (R_n C_m^{1/2}) + 0.03$$

Figure 3 shows a comparison of the Goldstein formula with the experimental data of Schmidt,[5] Kempf,[4] and Regier and Theodorsen.[6]

Schlichting[1] discussed the flow on rotating bodies. According to Schlichting, the boundary layer thickness for the laminar case was proportional to $(\nu/\omega)^{1/2}$; for the turbulent boundary layer, to $(\nu/\omega)^{1/5}$. The axial inflow velocity is proportional to $(\nu\omega)^{1/2}$.

Dorfman[8] presented a collection of investigations of rotating-disk flow by von Karman, Cochran, and Goldstein. Dorfman analyzed the turbulent flow due to a rotating disk for disks with both smooth and rough surfaces. For the disk with a smooth surface, Dorfman used a logarithmic velocity distribution and found the moment coefficient to be $C_m = 0.982(\log R_n)^{-2.58}$. For the disk with a rough surface and a fully turbulent boundary layer, Dorfman found the moment coefficient to be

$$C_m = 0.108 (k_s/R)^{0.272}$$

---

[7]Goldstein, S., "On the Resistance to the Rotation of a Disc Immersed in a Fluid," Proceedings of the Cambridge Philosophical Society 31, pp. 232-241 (1935).

[8]Dorfman, L.A., "Hydrodynamic Resistance and the Heat Loss of Rotating Solids," Oliver and Boyd, First Edition, pp. 1-71 (1963).

where k_s is the characteristic roughness height. The characteristic roughness height is defined as the height at which uniformly graded sand grains will project above the smooth surface.

EXPERIMENTAL

Kempf[4] measured the torque of rotating disks in air. The surfaces considered were polished brass, wood with finely polished lacquers, and finely smooth paraffin surface. The Reynolds numbers considered were 1×10^4 to 2×10^6. The disk was driven by a weight and pulley arrangement, torque being measured by torsion springs. For $R_n < 8 \times 10^4$, C_m approaches the theoretical curve of von Karman for the turbulent boundary layer. The Kempf data are also presented in Figure 3.

Theodorsen and Regier[6] obtained experimentally the moment coefficient as a function of the Reynolds number from $R_n = 3.96 \times 10^3$ to $R_n = 1.58 \times 10^6$ for a rotating disk; see Figure 3. The moment was found by relating the torque to the horsepower required to drive the disk at a specified angular velocity.

EXPERIMENTAL TECHNIQUE

APPARATUS

The rotating-disk apparatus (Figure 4a) was mounted in a cylindrical steel tank 5 ft in height and 5.5 ft in diameter for experiments in air and in water; see Figures 4b and 4c. The power to rotate the steel disk, 1-ft R and 3/16 in. thick, was supplied by a Variac controlled electric motor. A variable reluctance-transmission dynamometer connected the disk by an arrangement of shaft, bearing, and coupling; Figure 5. Figure 6 shows the flexible coupling connecting the disk shaft to the dynamometer. A magnetic pickup-toothed gear configuration (Figure 4a) determined the angular velocity of the disk.

The changes in magnetic intensity caused by the gaps in a rotating-toothed gear were counted with a Hewlett-Packard counter. This toothed-gear pickup was checked with a Strobotac.

The output signal of the dynamometer was demodulated through a Carrier dual channel demodulator and was displayed on a digital voltmeter. The steadiness of the torque was determined by a single channel Sanborn

Figure 4 - Rotating-Disk Apparatus

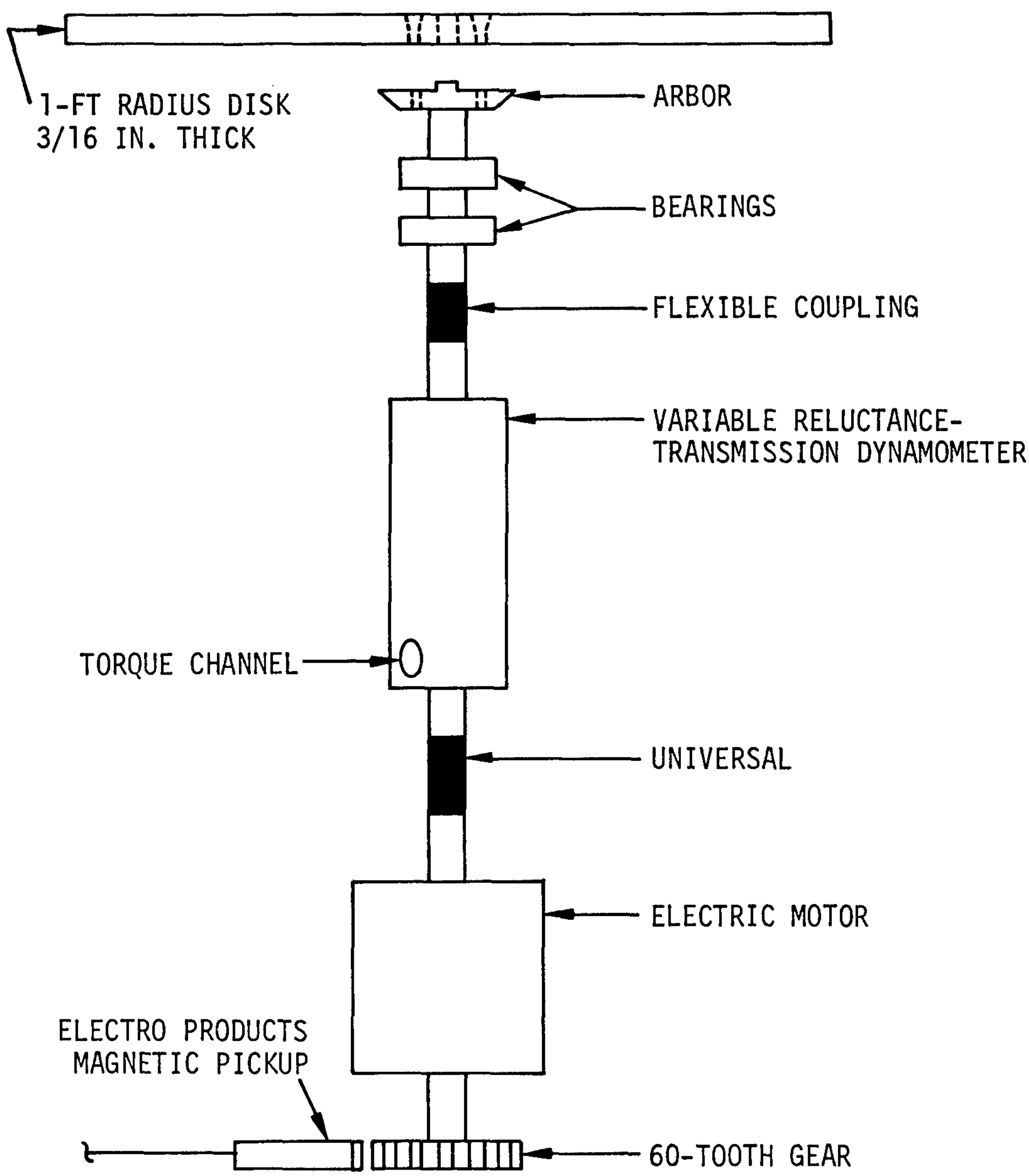

Figure 4a - Side View

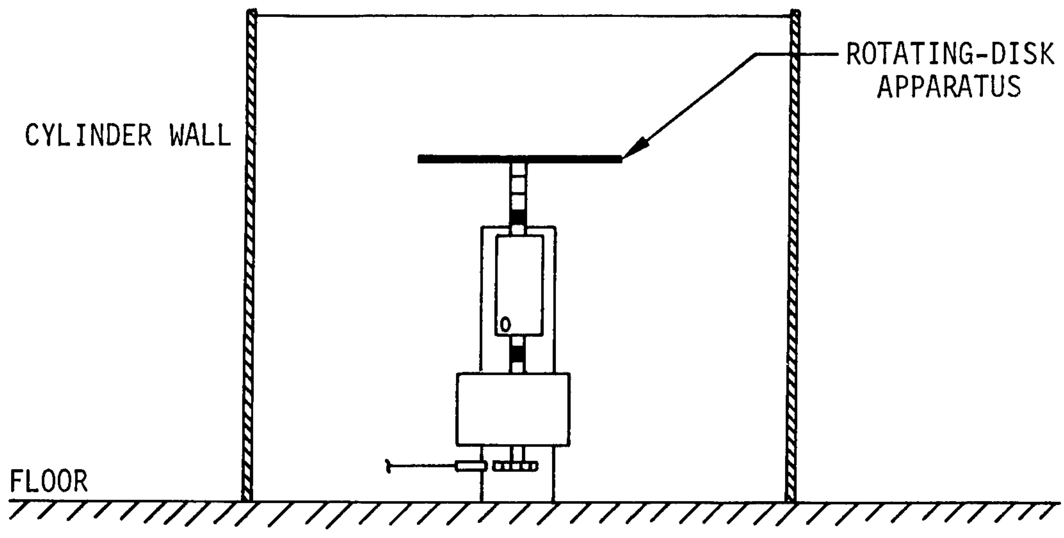

Figure 4b - Mounted in Cylindrical Tank for Air Tests

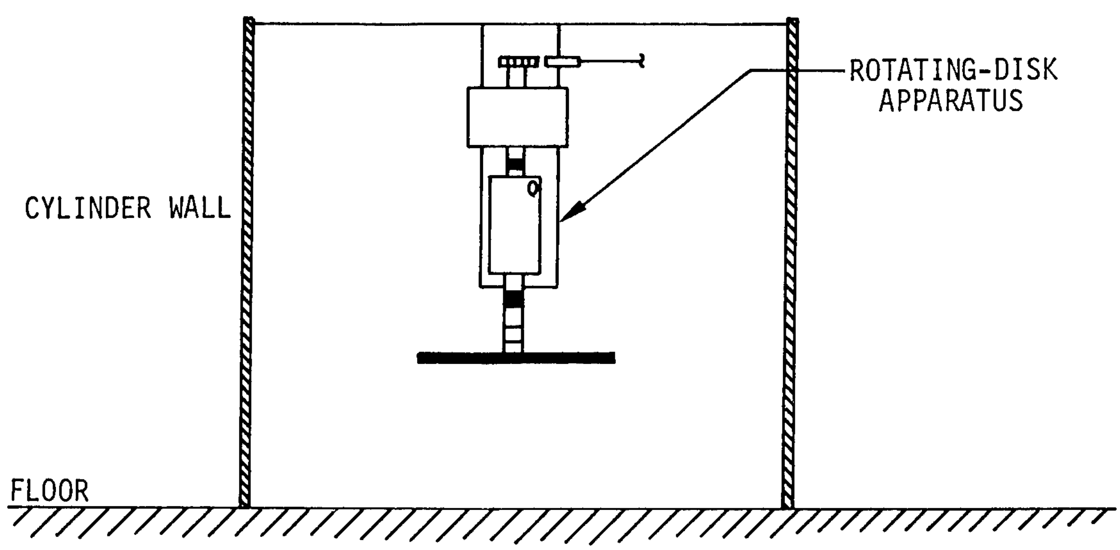

Figure 4c - Mounted in Cylindrical Tank for Air
and Water Tests

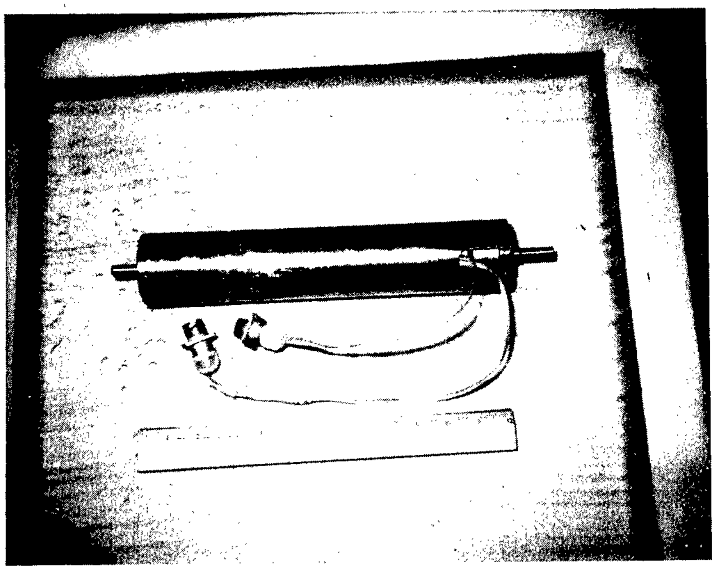

Figure 5 - Variable Reluctance-Transmission Dynamometer-
Torque and Thrust Cables Shown

Figure 6 - Flexible Coupling Connecting Disk Shaft to Dynamometer Shaft

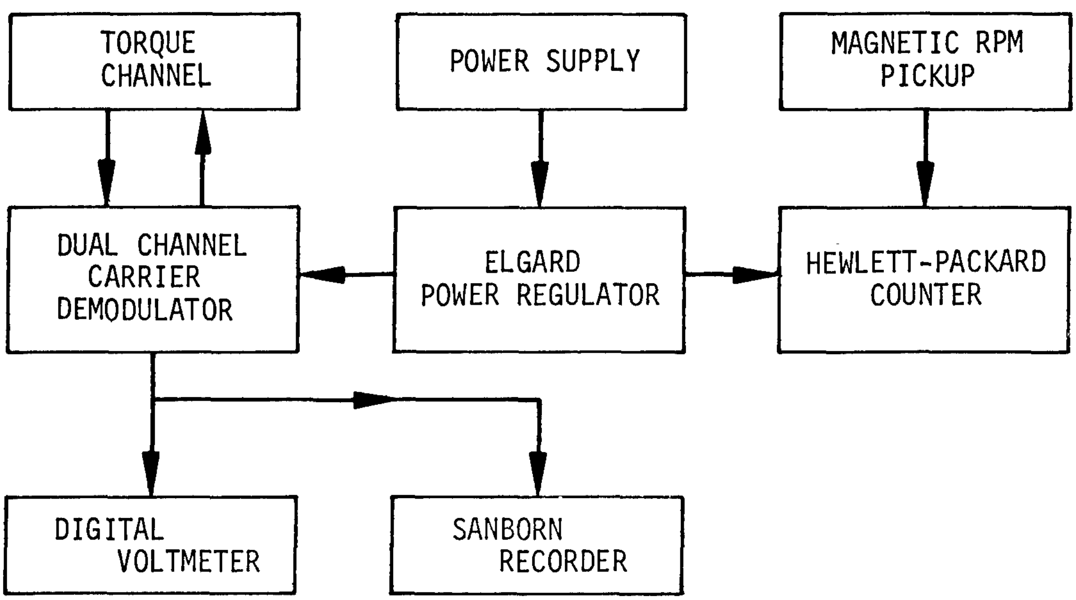

Figure 7 - Rotating-Disk Instrumentation

recorder. The power to the Carrier dual channel demodulator, the digital voltmeter, and the Hewlett-Packard counter was regulated by an Elgard power regulator. Figure 7 shows the rotating-disk instrumentation.

CALIBRATION

The dynamometer was calibrated statically on the stand shown in Figure 8. It consisted of brackets, and electric motor, and lever arrangements that could apply both torque and thrust on the dynamometer. The dynamometer was allowed to "warm up" by rotating the dynamometer shaft for one or more hours before the calibration was performed. The resolution of the dynamometer was set by placing a known torque on the dynamometer and setting the span channel on the Carrier dual channel demodulator for a chosen millivolt output displayed on the digital voltmeter. For example, if a torque of 10 in.-lb was applied to the dynamometer shaft, the span was set at 500mV, the resolution would be 50 mV/in.-lb. The torque gage was calibrated in both clockwise and counterclockwise directions.

DISK SURFACES

Two disk surfaces were evaluated in air, and one disk surface was evaluated in water. The smooth-surfaced disk for the air and water experiments was machined to a 63 finish. This represents a root-mean-square roughness height of 63 μin. For a 1-ft R, a 63 finish represents a $k_s/R = 0.0000525$. The rough-surfaced disk used for air experiments only was composed of 36 jewell garnet sandpaper. The number 36 represents sand-grain size and is characterized in Table 1. Using Table 1, a characteristic roughness height of 0.0232 in. was calculated for the rough surface of the disk because 80 to 100 percent had to pass through Sieve 30 but 45 to 100 percent had to be retained on Sieve 35.

PROCEDURE

The torque, as a function of the angular velocity of the disk, was found for a 1-ft R rotating in air and in water. The disk surfaces evaluated were smooth and sandpaper rough for the disk rotating in air. For the disk rotating in water, only the smooth surface was investigated. The output of the dynamometer was displayed on a digital voltmeter so that the average torque could be determined. A Sanborn recorder was used to determine the unsteady dynamometer torque output.

Figure 8 - Dynamometer-Calibration Apparatus

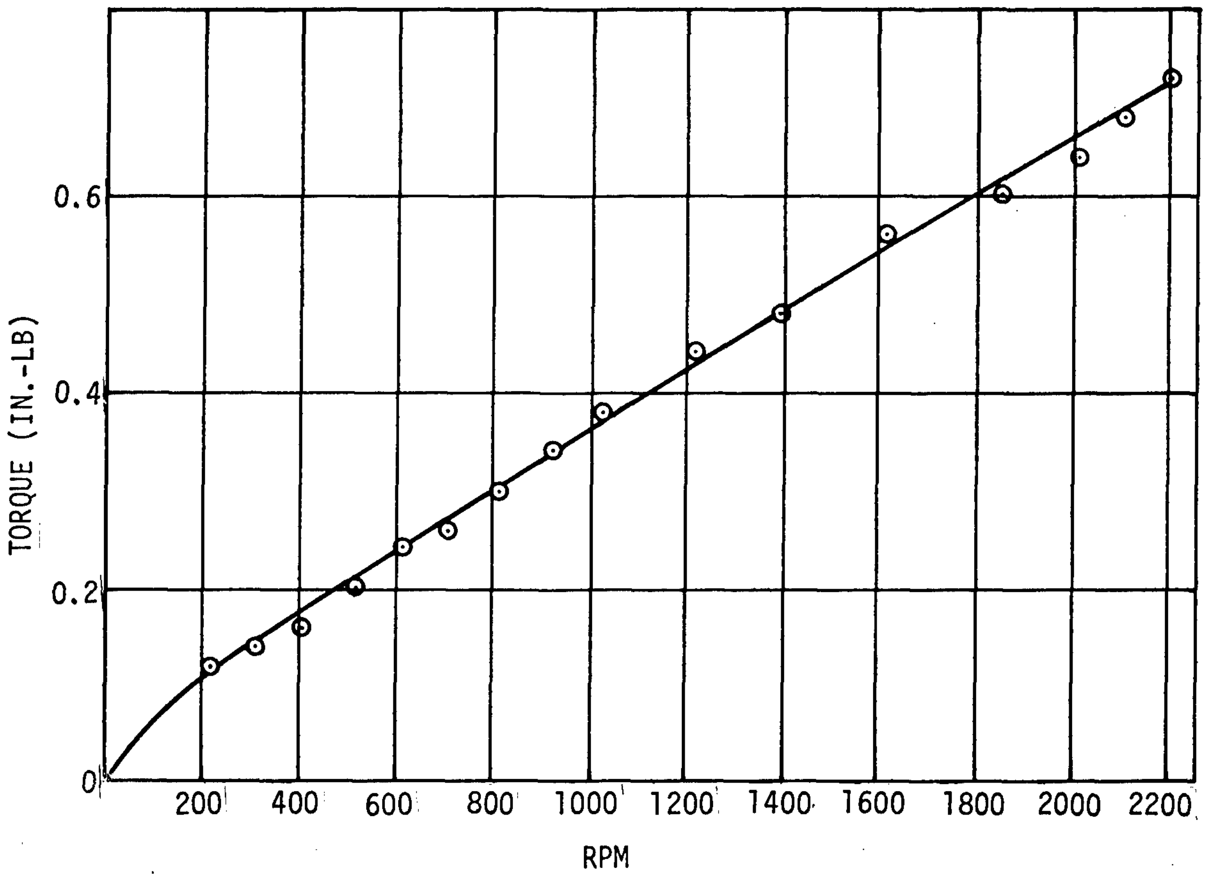

Figure 9 - No-Disk Torque as a Function of Revolutions per Minute

TABLE 1 - GRAIN SIZES AND U.S. STANDARD SIEVE SERIES*

Abrasive Grain Sizes and United States Standard Sieve Series
Approved by Abrasive Grain Association and Grinding Wheel Manufacturers Association

Allowable Size Limits for Aluminum Oxide and Silicon Carbide Abrasives for Polishing Uses and Grinding-wheels.

Grit No.	100 % Must Pass Sieve No. Below	Control Sieve		Max. % of Oversize on Control Sieve	Min. Through Control Sieve and Retained		Cumulative Min. Through Control Sieve and Retained		Max. of 3% to Pass Sieve No.
		No.	Opening Inch		%	On Sieve No.	%	On Sieve No.	
10	7	8	0.0937	15	45	10	80	10 and 12	14
12	8	10	0.0787	15	45	12	80	12 and 14	16
14	10	12	0.0661	15	45	14	80	14 and 16	18
16	12	14	0.0555	15	45	16	80	16 and 18	20
20	14	16	0.0469	15	45	18	80	18 and 20	25
24	16	20	0.0331	20	45	25	75	25 and 30	35
30	18	25	0.0280	20	45	30	75	30 and 35	40
36	20	30	0.0232	20	45	35	75	35 and 40	45
46	30	40	0.0165	20	45	45	75	45 and 50	60
54	35	45	0.0138	20	45	50	75	50 and 60	70
60	40	50	0.0117	30	45	60	65	60 and 70	80
70	50	60	0.0098	15	45	70	70	70 and 80	100
80	60	70	0.0083	15	40	80	70	80 and 100	120
90	70	80	0.0070	15	40	100	70	100 and 120	140
100	80	100	0.0059	15	40	120	65	120 and 140	200
120	100	120	0.0049	15	30	140	60	140 and 170	230
150	100	140	0.0041	15	40	170 and 200	75	170, 200 and 230	270
180	120	170	0.0035	15	40	200 and 230	65	200, 230 and 270	....
220	140	200	0.0029	15	40	230 and 270	60	230, 270 and 325	....

To illustrate, take grit No. 10. All material must pass through the coarsest sieve — in this case the No. 7. Through the next to the coarsest sieve, termed the "control sieve" — in this case the No. 8 — all material may pass, but not more than 15 per cent may be retained on it. At least 45 per cent must pass through No. 8, and be retained on No. 10 sieve, but it is permissible to have 100 per cent pass through No. 8, and remain on No. 10 sieve, the requirement being that the grain passing through No. 8, and retained on No. 10 and No. 12 must add to at least 80 per cent; consequently, if 45 per cent passed through No. 8 sieve and was retained on No. 10 sieve, then at least 35 per cent must be retained on the No. 12 sieve. Not more than 3 per cent is permitted to pass through the No. 14 sieve.

United States Standard Sieve Series

U. S. Standard Sieve Series No.	Sieve Opening		Sieve Wire Diam., Inch
	mm.	Inch	
4	4.76	0.187	0.050
5	4.00	0.157	0.044
6	3.36	0.132	0.040
7	2.83	0.111	0.036
8	2.38	0.0937	0.0331
10	2.00	0.0787	0.0299
12	1.68	0.0661	0.0272
14	1.41	0.0555	0 0240
16	1.19	0.0469	0.0213
18	1.00	0.0394	0.0189
20	0.84	0.0331	0.0165
25	0.71	0.0280	0.0146
30	0.59	0.0232	0.0130
35	0.50	0.0197	0.0114
40	0.42	0.0165	0.0098
45	0.35	0.0138	0.0087
50	0.297	0.0117	0.0074
60	0.250	0.0098	0.0064
70	0.210	0.0083	0.0055
80	0.177	0.0070	0.0047
100	0.149	0.0059	0.0040
120	0.125	0.0049	0.0034
140	0.105	0.0041	0.0029
170	0.088	0.0035	0.0025
200	0.074	0.0029	0.0021
230	0.062	0.0024	0.0018
270	0.053	0.0021	0.0016
325	0.044	0.0017	0.0014

---

*Oberg, E., and Jones, F.D., "Machinery Handbook - 12 Edition," 1945

The system was run at various angular velocities without the disk to determine the effect of bearing friction on the dynamometer output. At high angular velocities this no-disk torque was significant and had to be subtracted from later dynamometer output readings when the disk was attached. Figure 9 shows no-disk or bearing-friction torque. The data with the disk in the system were taken in the following manner.

1. The dynamometer reading was taken on the digital voltmeter for the disk at zero angular velocity.

2. The disk was accelerated and allowed to achieve a steady angular velocity.

3. When the angular velocity was constant, a reading from the digital voltmeter was taken.

4. The disk was then accelerated to a higher angular velocity and was allowed to reach a steady value. After a few minutes, a reading from the digital voltmeter was again taken.

5. Steps 2 through 4 were repeated until the torque limit of the dynamometer was reached.

6. After all the data had been taken, the motor was turned off. When the disk had stopped rotating, readings were again taken to ascertain any zero shift during the run.

When measuring the torque for a given angular velocity, it was necessary to have a true zero reading. Initially a rigid steel coupling connected the disk and the dynamometer shafts; however, this system would not return to a zero reading after a torque measurement had been taken. To insure proper zero readings after a measurement had been taken, the flexible coupling (Figure 6) was installed. For the experiments in air, the smooth-surfaced disk was rotated at two positions, 18 in. from the open end of the cylindrical tank and 18 in. from the closed end. In air, the rough-surfaced disk was rotated 18 in. from the open end only. For the water experiments, the smooth-surfaced disk only was rotated 18 in. from the closed end of the tank with the water levels above the disk at heights of 1, 3, 5, and 7 in.

RESULTS AND DISCUSSION

The results of the torque measurements in air and in water are presented in Figures 10 through 15 and Table 2.

An error analysis of the moment coefficient and Reynolds number is presented in Appendix B. The moment coefficient error ranged from 2 to 12 percent; the Reynolds number error ranged from 2 to 2.5 percent. Possible errors could be due to inaccuracy in measuring the fluid density, disk radius, angular velocity, and disk torque. The measured torque includes both bearing-friction and disk torques. Thus, the average torque due to the disk only is $T_{disk} = T_{measured} - T_{bearing\ friction}$. Any error in torque would probably be due to a change in $T_{bearing\ friction}$ since this torque depends on bearing lubrication which may vary with time and rpm.

BEARING-FRICTION TORQUE

Figure 10 shows the unsteady bearing-friction torque (no-disk) at 2000 rpm. Figure 11 shows the unsteady torque for the disk rotating at 1976 rpm. Comparison of Figures 10 and 11 seems to indicate that the unsteady torque is mainly due to the unsteadiness of the bearing friction.

EFFECT OF HOUSING

Since the disk was not rotated in an infinite viscous fluid, the effect of the fluid boundaries had to be determined. Figure 12 shows a comparison between torques for the disk rotating in air at the open and the closed ends of the steel housing. Torque appeared to be greater at the higher angular velocities when the disk was rotated in a relatively unbounded viscous fluid. For the water experiments, no similar test could be made with the disk apparatus used in this experiment.

EFFECT OF WATER DEPTH

For the disk rotating in water, two effects were determined by measuring the torque due to the disk at various water depths. The water-depth measurements took into account the surface-movement effect and the effect of the fluid boundaries. For the water experiments, these two effects could not be determined separately.

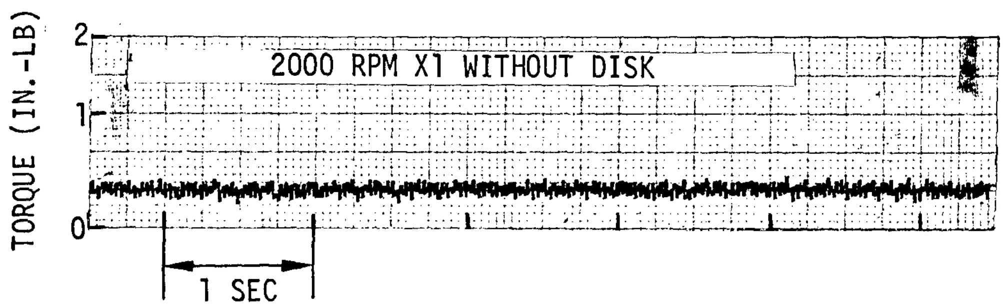

Figure 10 - Unsteady No-Disk Torque for Dynamometer Shaft Rotating in Air at 2000 Revolutions per Minute

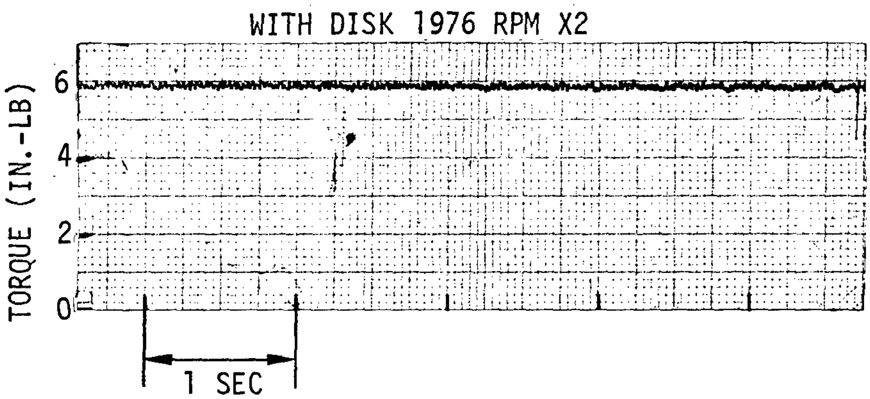

Figure 11 - Unsteady Torque of Disk Rotating in Air at 1976 Revolutions per Minute

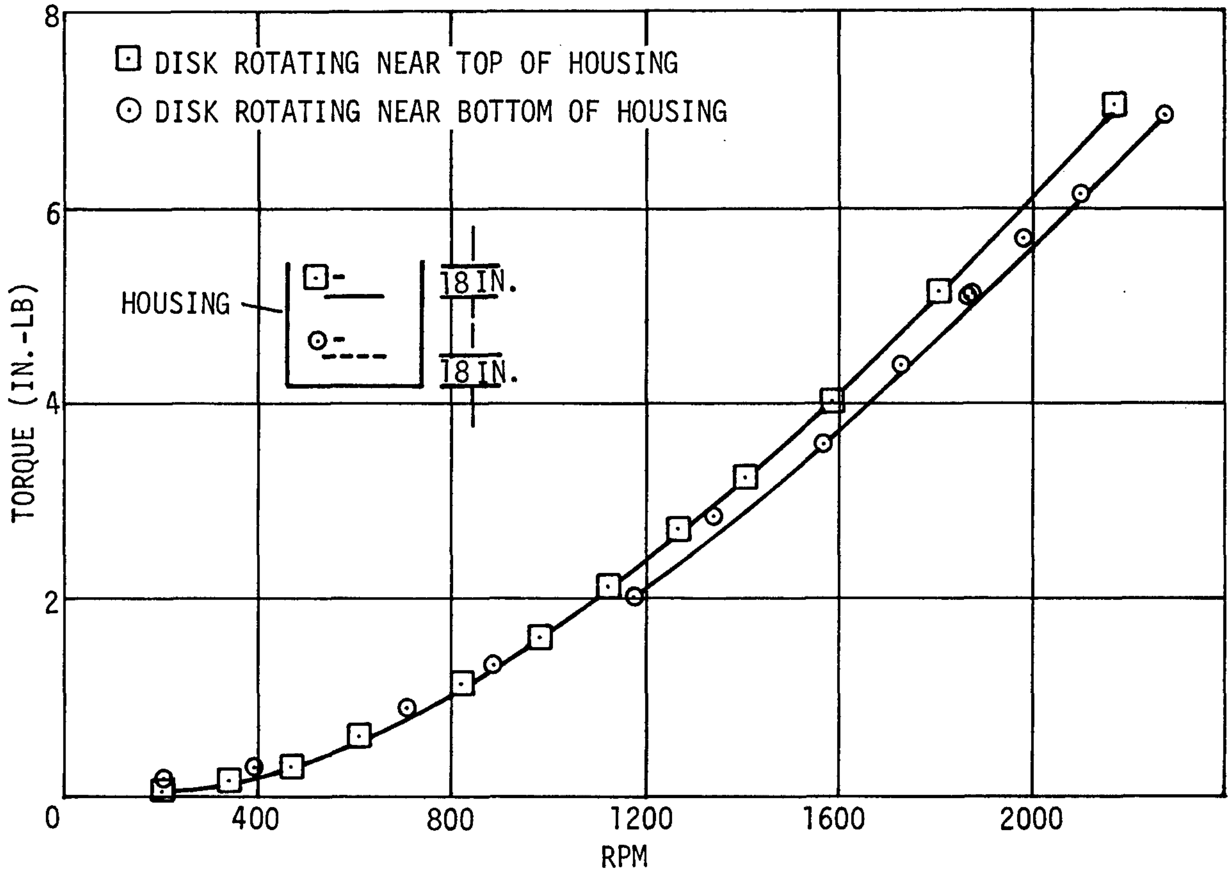

Figure 12 - Effect of Steel Housing on Torque Due to a Disk Rotating in Air

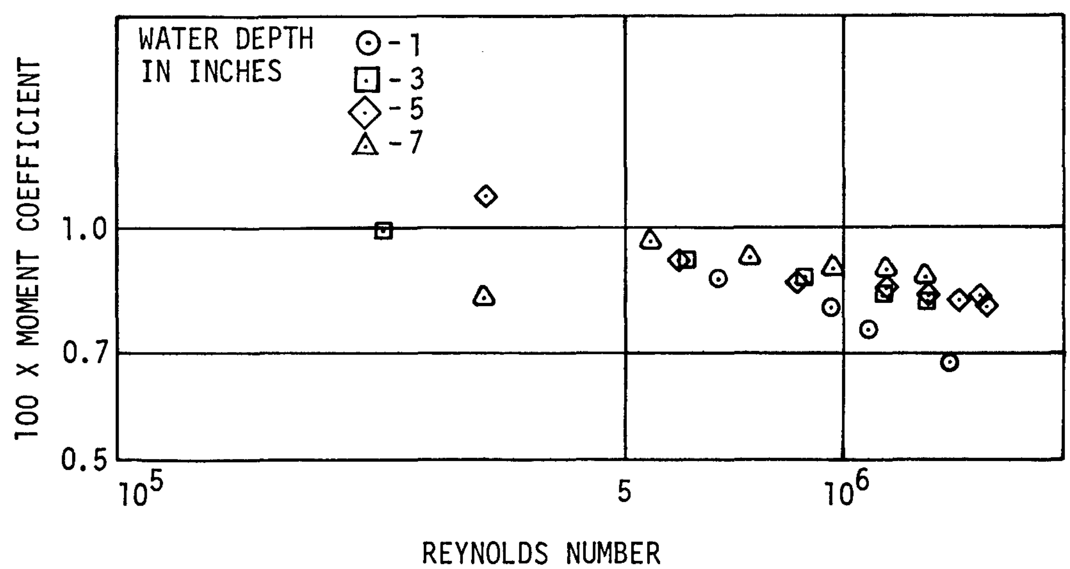

Figure 13 - Effect of Water Depth on Torque Due to a Disk Rotating in Water

Figure 14a - Disk Rotating at 100 Revolutions per Minute

Figure 14b - Disk Rotating at 170 Revolutions per Minute

Figure 14 - Surface Effects of a Disk Rotating at 100 and 170 Revolutions per Minute at a Disk Depth of 5 Inches

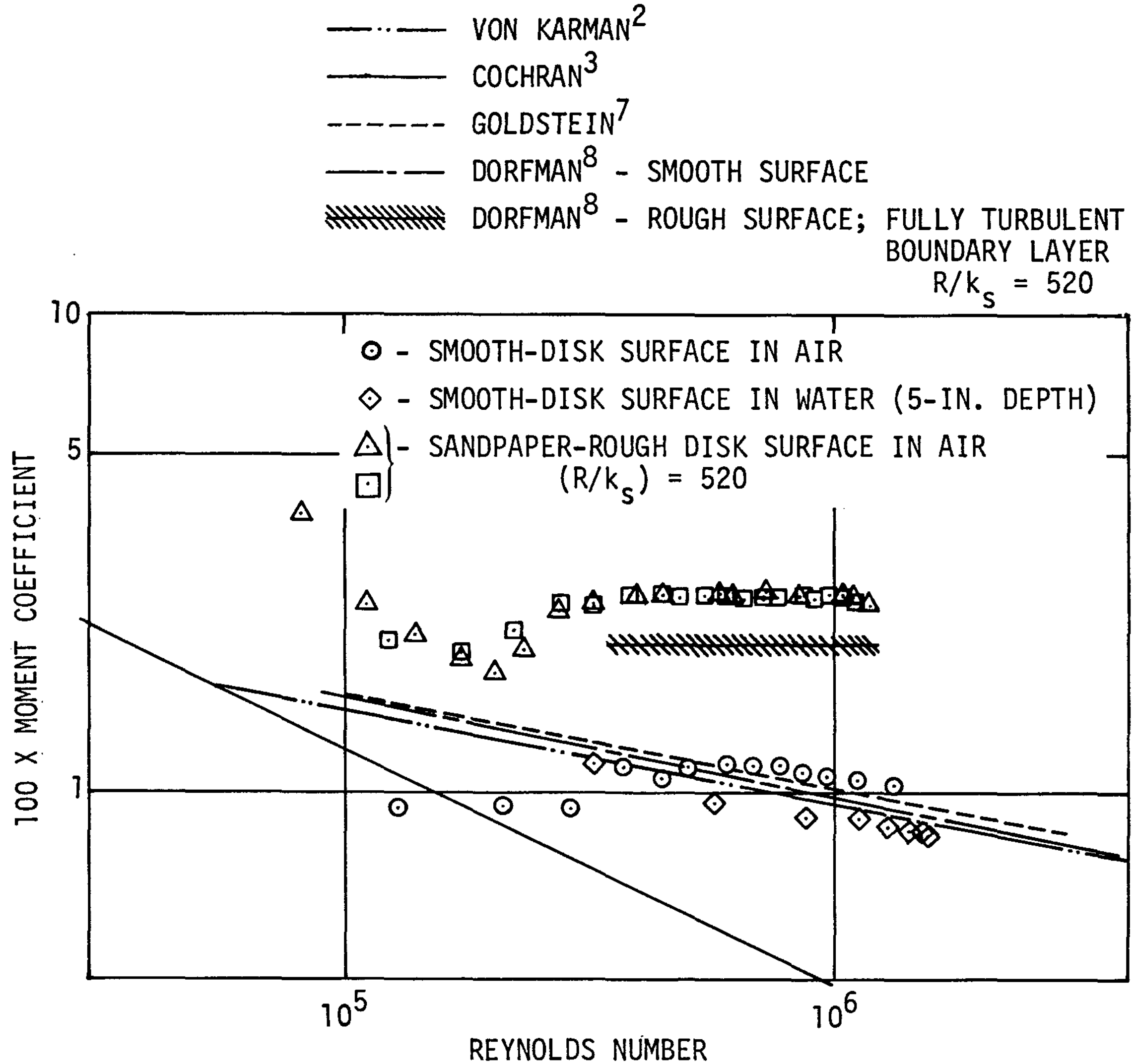

Figure 15 - Experimental Results of Moment Coefficient as a Function of Reynolds Number for a Disk Rotating in a Viscous Fluid Initially at Rest

For the disk in water, the effect of the water depth on the moment coefficient was found; see Figure 13. The trend was a decreasing torque for a decreasing water depth. This was probably due to the increased surface movement which would tend to give the fluid a lower velocity relative to the disk and thus a lower torque.

Photographs of the water surface for the disk rotating at 100 and 170 rpm are shown in Figure 14. The disk is at a depth of 5 in. from the water surface and 18 in. from the bottom of the tank.

EFFECT OF THE DISK EDGE

The data presented in Figure 15 include the effect of the disk edge. From Dorfman,[8] the moment coefficient excluding the effect of the edge is as follows

$$C_m = C_m'/(1 + 2.5\ b/R)$$

where C_m' is moment coefficient due to disk and its edge

C_m is moment coefficient due to disk only

b is thickness of disk or 3/16 in.

R is radius of disk or 12 in.

For the disk used in this investigation, the value of b/R is 0.0156. Thus

$$C_m = \frac{C_m'}{1 + 2.5(1/64)} = \frac{C_m'}{1 + 0.0391} = 0.96\ C_m'$$

The torque due to the disk only is 96 percent of the torque due to the disk and its edge.

MOMENT COEFFICIENT AS A FUNCTION OF REYNOLDS NUMBER

The theoretical analyses of Goldstein, von Karman, and Dorfman assumed that the turbulent boundary layer existed at all disk radii. This is not the case for there exist three boundary-layer flows on the disk--laminar, transitional, and turbulent. Thus, the experimental and theoretical results may differ. The type of disk, surface roughness, tested and the method of measuring the torque are two more variables that would effect the experimental moment-coefficient results.

Table 2 is a comparison of experimental and theoretical results. The errors associated with experimental results by the author are also

TABLE 2 - COMPARISON OF EXPERIMENTAL ROTATING-DISK, SMOOTH-SURFACE MOMENT-COEFFICIENT RESULTS WITH THEORETICAL RESULTS OF GOLDSTEIN AND VON KARMAN

Reynolds Number $\times 10^{-5}$	$C_m' \times 10^2$ Moment Coefficient (Disk and Edge)	$C_{m_E} \times 10^2$ Moment Coefficient (Disk only)	Percent Error in C_m' Measurement	$C_{m_G} \times 10^2$ Goldstein Moment Coefficient	$\frac{C_{m_G} - C_{m_E}}{C_{m_G}}$	$C_{m_V} \times 10^2$ von Karman Moment Coefficient	$\frac{C_{m_V} - C_{m_E}}{C_{m_V}}$
1.29	0.916	0.879	35	1.454	0.395	1.386	0.366
2.10	0.929	0.892	14	1.331	0.329	1.258	0.291
2.90	0.915	0.878	8	1.257	0.301	1.180	0.256
3.77	1.122	1.077	5	1.201	0.103	1.120	0.038
4.42	1.069	1.026	4	1.169	0.122	1.085	0.054
5.08	1.116	1.071	3	1.142	0.062	1.055	-0.015
6.08	1.143	1.097	2.4	1.109	0.011	1.018	-0.078
6.94	1.132	1.087	2.1	1.085	-0.002	0.991	-0.097
7.88	1.119	1.074	1.9	1.062	-0.011	0.996	-0.078
8.71	1.099	1.055	1.7	1.045	-0.009	0.947	-0.114
9.83	1.071	1.028	1.5	1.025	-0.003	0.924	-0.113
11.18	1.054	1.012	1.4	1.005	-0.007	0.901	-0.123
13.39	1.010	0.970	1.3	0.977	+0.007	0.869	-0.116

shown in Table 2. Agreement of experimental results with the theory of Goldstein is good for Reynolds number greater than 6.08×10^5.

The theoretical results of Goldstein were based on the experimental results of Schmidt and Kempf. No error analysis of their experimental data was presented in References 4 and 5. The theoretical results of von Karman were based strictly on fluid-boundary conditions and the one-seventh power velocity distribution.

The smooth-surface torque data in air from a disk rotated near the top of a cylindrical tank are shown in Figure 15 to be slightly higher than the theoretical curve of Goldstein for a turbulent boundary layer. The higher moment coefficient of Figure 15 is probably due to the influence of the disk edge. The smooth-surface data in water are slightly lower than the theoretical, turbulent boundary-layer result of von Karman. For the disk in water, both the disk-edge and the water-depth effects must be considered. For a given Reynolds number, the moment coefficient due to the disk and its edge is greater than the moment coefficient due to the disk only. For the disk in water (Figure 13), for a given Reynolds number as the depth increased, the moment coefficient increased. Since the maximum depth at which the disk was tested was 7 in., the disk was not rotated in an infinite fluid. Thus a lower moment coefficient would result. If this finite water-depth effect were to dominate the disk-edge effect, a moment coefficient lower than the theoretical value might result.

The theoretical moment coefficient for the rough disk was calculated from the Dorfman equation for a rough surface[8] with a ratio of sandpaper radius to roughness height of 520 or 36 grit sandpaper. This calculation yields

$$C_m = 0.108(k_s/R)^{0.272}; \; k_s = 0.00193 \text{ feet} \quad \text{or} \; \frac{R}{k_s} = 520$$

$$R = 1 \text{ foot}$$

therefore

$$C_m = 0.02$$

whereas the results of Figure 15 for the disk near top of cylindrical tank indicates a $C_m = 0.025$. Theodorsen and Regier data yield a $C_m = 0.02$ for $R/k_s = 1215$; however, using this value of (R/k_s) with the Dorfman equation yields $C_m = 0.015$. The rough surface C_m of Figure 3 and Figure 15 are higher than those calculated by using the Dorfman equation, which could partially be due to the fact that the Dorfman equation does not allow for the effect of the disk edge. Thus, if the effects of the disk edge and the water depth were taken into account, the data presented in Figure 15 would better agree with the various theoretical results.

As can be seen in Table 2, with disk-edge effects neglected, the Goldstein theoretical results for a smooth-surfaced disk agree most favorably with the experimental results by the author for $R_n > 6.08 \times 10^5$.

CONCLUSIONS

The following conclusions have been drawn from the present investigation.

1. The present rotating-disk apparatus cannot simulate full-scale-ship Reynolds number.
2. Bearing-friction torque must be reduced or eliminated to reduce the error in the torque measurements.
3. Fluid boundary and disk-edge effects are significant and must be accounted for when comparing experimental results with theory.

RECOMMENDATIONS

The rotating-disk apparatus could be improved by making the following modifications.

1. Devise a system that would reduce or eliminate the bearing-friction torque. This would decrease the error in the torque measurement.
2. Characterize the disk roughness height in a standard manner; i.e., root mean square or average values. This would allow for consistent comparison of results.
3. Construct a waterproof tank. The cylindrical tank was not waterproof and had to be lined with plastic liner for the water tests. This arrangement was very awkward.
4. Modify the present apparatus so that water tests can be done for greater water depths above and/or below the disk. This modification will help to reduce the free-surface effect.
5. Increase both disk diameter and angular velocity so that full-scale-ship Reynolds number can be attained.

ACKNOWLEDGMENTS

The author wishes to acknowledge the assistance of Messrs. C.W. Geib, J.J. Gordon, H.D. Harper, and L.B. Moore for their preparation of the instrumentation system.

APPENDIX A

FORCE BALANCE

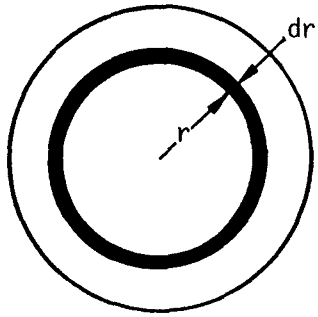

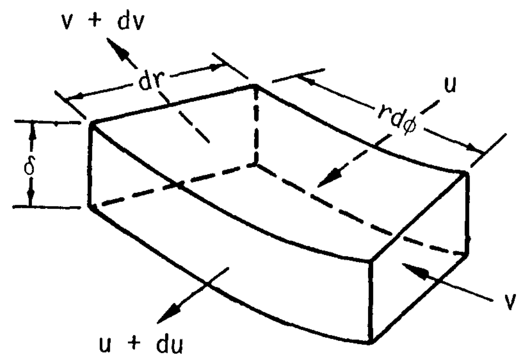

Disk with Ring of Fluid Element

Fluid Element

Application of the steady-state momentum equation in the radial direction to an element of fluid thickness δ yields

$$dF_c + dF_s = \int_o^\delta \rho(u + du)^2 \,[2\pi(r + dr)dz] - \int_o^\delta \rho u^2 \,(2\pi r\, dz)$$

where $dF_c = 2\pi r \left[\rho \int_o^\delta \frac{v^2}{r}\, dz\right]$ dr is the centrifugal force since $dv = 0$

$dF_s = -\, 2\pi r\, \tau_r\, dr$ is the shear force

where ρ is density of fluid, and τ_r is shear in radial direction. For this force-balance analysis,[8] $p = p(z)$ is assumed. If higher order terms are neglected, the steady-state momentum equation in the radial direction simplifies to

$$dF_c + dF_s = \int_o^\delta 2\pi\rho\,(2ur\,du + u^2 dr)\,dz = \int_o^\delta 2\pi \frac{d(u^2 r)}{dr}\, dr\, dz$$

or

$$dF_s = \frac{d}{dr}\left(2\pi r\rho \int_o^\delta u^2 dz\right) dr - dF_c$$

Application of the steady-state angular momentum equation in the circumferential direction to an element of fluid thickness δ yields

$$- dM = \int_0^\delta \rho(u + du)\ (v + dv)\ 2\pi(r + dr)^2\ dz - \int_0^\delta \rho uvr^2\ 2\pi\ dz$$

where $- dM = - \tau_\phi(2\pi r^2)\ dr$ is the moment on an element around the center of the disk, and τ_ϕ is shear in the circumferential direction. If higher order terms are neglected, the steady-state momentum equation in the circumferential direction simplifies to

$$-\tau_\phi\ (2\pi r^2)dr = \int_0^\delta 2\pi\rho r^2 \frac{d(uv)}{dr}\ dr\ dz$$

or

$$\frac{d}{dr}\ r^2 \int_0^\delta uvdz = - \frac{\tau_\phi r^2}{\rho}$$

APPENDIX B

ERROR ANALYSIS

An error analysis of the moment coefficient and Reynolds number is presented

$$\text{Moment Coefficient: } C_m = \frac{T}{1/2\ \rho\omega^2 R^5} \tag{9}$$

where T is the torque due to both sides of the disk. The logarithmic form of Equation (9) is

$$\log C_m = \log T - \log (1/2) - \log \rho - 2 \log \omega - 5 \log R \tag{10}$$

The derivative of Equation (10) yields

$$\frac{dC_m}{C_m} = \frac{dT}{T} - \frac{d\rho}{\rho} - \frac{2d\omega}{\omega} - \frac{5dr}{R}$$

The quantity $\frac{dC_m}{C_m}$ represents the error in the moment coefficient. For maximum error, either all signs are positive or all signs are negative. If all positive signs are assumed

$$\frac{dC_m}{C_m} = \frac{dT}{T} + \frac{d\rho}{\rho} + \frac{2d\omega}{\omega} + \frac{5dr}{R} \tag{11a}$$

or

$$\frac{\Delta C_m}{C_m} = \frac{\Delta T}{T} + \frac{\Delta\rho}{\rho} + \frac{2\Delta\omega}{\omega} + \frac{5\Delta R}{R} \tag{11b}$$

where $\Delta T = 0.02$ in.-lb

$\Delta\rho = 0.00002$ lbf-sec^2/ft^4

$\Delta\omega = 1$ rpm

$\Delta R = 0.0002$ ft

$\rho = 0.00225$ lbf-sec^2/ft^4

$R = 1$ ft

For $T = 0.2$ in.-lb and $\omega = 200$ rpm

$$\frac{\Delta C_m}{C_m} = \frac{0.02}{0.20} + \frac{0.00002}{0.00225} + \frac{2}{200} + \frac{0.001}{1}$$

$$\frac{\Delta C_m}{C_m} \approx 0.12$$

For T = 4 in.-lb, and ω = 1600 rpm

$$\frac{\Delta C_m}{C_m} = \frac{0.02}{4} + \frac{0.00002}{0.00225} + \frac{2}{1600} + \frac{0.001}{1}$$

$$\frac{\Delta C_m}{C_m} \approx 0.02$$

Therefore, for low torque measurements, the maximum moment coefficient error is approximately 12 percent. For high torque measurements, the maximum moment coefficient error is approximately 2 percent.

$$\text{Reynolds Number: } R_n = \frac{\omega R^2}{\mu/\rho} \qquad (12)$$

The logarithmic form of Equation 12 is

$$\log R_n = \log \omega + 2 \log R + \log \rho - \log \mu \qquad (13)$$

The derivative of Equation (13) yields

$$\frac{dR_n}{R_n} = \frac{d\omega}{\omega} + \frac{2dR}{R} + \frac{d\rho}{\rho} - \frac{d\mu}{\mu}$$

The quantity $\frac{dR_n}{R_n}$ represents the error in the Reynolds number. For maximum error all signs are positive

$$\frac{dR_n}{R_n} = \frac{d\omega}{\omega} + \frac{2dR}{R} + \frac{d\rho}{\rho} + \frac{d\mu}{\mu}$$

$$\frac{\Delta R_n}{R_n} = \frac{\Delta\omega}{\omega} + \frac{2\Delta R}{R} + \frac{\Delta\rho}{\rho} + \frac{\Delta\mu}{\mu}$$

$\mu = 3.83 \times 10^{-7} \qquad \Delta\mu = 0.04 \times 10^{-7}$

For ω = 200 rpm

$$\frac{\Delta R_n}{R_n} = \frac{1}{200} + \frac{0.0004}{1} + \frac{0.00002}{0.00225} + \frac{0.04}{3.83}$$

$$\frac{\Delta R_n}{R_n} \approx 0.025$$

For ω = 1600 rpm

$$\frac{\Delta R_n}{R_n} \approx 0.02$$

Therefore, the maximum error in the Reynolds number is approximately 2.5 percent.

INITIAL DISTRIBUTION

Copies		Copies	
3	CHONR 2 Code 438 1 Code 472	5	NAVUSEACEN Pasadena 1 J.W. Hoyt 1 P.R. Kenis 1 J.G. Waugh 1 W.D. White
1	ONR BOSTON A. Wood	1	NAVWPNSCEN
2	NRL 1 R.C. Little	6	NOL 1 V.C. Dawson 1 A. May 1 A.E. Seigel 1 N. Tetervin 1 R.E. Wilson
2	CHNAVMAT 1 SP-11 1 SP-43	3	NPTLAB NUSC 1 P.E. Gibson 1 F.J. Brady 1 R.H. Nadolink
2	USNA 1 Bruce Johnson	1	NLONLAB NUSC
2	NAVPGSCOL 1 T. Sarpkaya	2	NAVSEC 1 SEC 6110-01 1 SEC 6136
1	USNROTC & NAVADMINU, MIT	12	DDC
1	NAVWARCOL	1	Library of Congress
9	NAVSHIPSYSCOM 2 SHIPS 2052 1 SHIPS 031 1 SHIPS 03411 1 SHIPS 03412 1 SHIPS 03413 1 SHIPS 03421 2 SHIPS 0372	1	MARAD
2	NAVAIRSYSCOM 1 AIR 5301	1	NASA HQS I.R. Schwartz
4	NAVORDSYSCOM 1 ORD 035 1 ORD 035B 1 ORD 054131	1	Bureau of Standards Hydraulic Lab
2	NAVAIRDEVCEN 1 J.R. Dale	1	Arizona State Univ N.S. Berman
1	NELC	1	Univ of Bridgeport E.M. Uram
3	NAVUSEACEN San Diego 1 A.G. Fabula 1 T. Lang	1	Brown Univ R.I. Tanner
		1	Univ of Calif at San Diego A. Ellis

Copies	
1	Cal Inst of Tech A.J. Acosta
1	Clemson Univ W.E. Castro
1	Colorado State Univ J.P. Tullis
1	Univ of Delaware A.B. Metzner
1	Univ of Florida E.R. Lindgren
2	Georgia Inst of Tech 1 P.G. Mayer 1 W.M. Newton
1	Harvard Univ F.H. Abernathy
1	Univ of Hawaii J.P. Craven
1	Univ of Illinois T.J. Hanratty
1	Iowa State Univ Iowa Inst of Hydr Res L. Landweber
1	Johns Hopkins Univ W.H. Schwarz
1	Univ of Kentucky A.H.P. Skelland
3	Univ of Maryland 1 Dirse Sallet 1 F. Buckley 1 C.L. Sayre
1	Univ of Massachusetts C.E. Carver, Jr.
4	Mass Inst of Tech 2 Dept of Ocean Eng 2 Dept of Chem Eng

Copies	
2	Univ of Michigan 1 Dept NAME 1 W.P. Graebel
3	Univ of Minnesota St. Anthony Falls Hydr Lab
1	Univ of Missouri Dept of Chem Eng
1	Univ of Notre Dame N.D. Sylvester
1	Ohio Northern Univ R.J. Glass
1	Ohio State Univ H.C. Hershey
1	Univ of Oklahoma Research Inst E.F. Blick
3	Penn State Univ Applied Research Lab 1 J.L. Lumley 1 R.E. Henderson
2	Purdue Univ 1 A.T. McDonald 1 D.E. Abbott
2	Univ of Rhode Island 1 F.M. White 1 T. Kowalski
2	Stanford Univ 1 E.Y. Hsu 1 S.J. Kline
2	Stevens Inst, Davidson Lab 1 A. Strumpf
1	Univ of Tennessee D.C. Bogue
1	Texas A&M Univ R. Darby

Copies	
1	Virginia Polytechnic Inst E.R. van Driest
1	Webb Institute
1	Univ of West Virginia W. Squire
2	Worchester Polytechnic Inst 1 L.C. Neale
1	SNAME
1	Boeing Co. W. Pfenninger
1	Esso Math & Systems Richard Bernicker
1	General Electric Company R & D Center W.B. Giles
6	Hydronautics 1 V. Johnson 1 Jin Wu 1 M.P. Tulin 1 D. Fruman 1 A. Gollan
1	LTV Advanced Tech Center C.S. Wells
1	Mobil Field Res Lab J.G. Savins
1	Oceanics A. Lehman
1	Union Carbide Corp F.W. Stone

CENTER DISTRIBUTION

Copies		
1	15	Cummins
1	1508	CDR Moran
1	152	Wermter
1	1528	Strom-Tejsen
1	154	Morgan
1	1541	Granville
20	1544	Cumming
1	1552	McCarthy
3	1556	Cieslowski
1	156	Hadler
1	2762	Howard
1	2833	Felsen

☆U.S. GOVERNMENT PRINTING OFFICE: 1973 542-164/Z-56 1-3

Unclassified
Security Classification

DOCUMENT CONTROL DATA - R & D

(Security classification of title, body of abstract and indexing annotation must be entered when the overall report is classified)

1. ORIGINATING ACTIVITY *(Corporate author)* Naval Ship Research and Development Center Bethesda, Maryland 20034	2a. REPORT SECURITY CLASSIFICATION Unclassified 2b. GROUP

3. REPORT TITLE

EVALUATION OF A ROTATING DISK APPARATUS: DRAG OF A DISK ROTATING IN A VISCOUS FLUID

4. DESCRIPTIVE NOTES *(Type of report and inclusive dates)*

Final

5. AUTHOR(S) *(First name, middle initial, last name)*

John J. Nelka

6. REPORT DATE	7a. TOTAL NO. OF PAGES	7b. NO. OF REFS
July 1973	46	8

8a. CONTRACT OR GRANT NO.	9a. ORIGINATOR'S REPORT NUMBER(S)
b. PROJECT NO. SR 009 01 01	3851
c. Task 0104	9b. OTHER REPORT NO(S) *(Any other numbers that may be assigned this report)*
d. Work Unit 1-1589-086	

10. DISTRIBUTION STATEMENT

Approved for Public Release: Distribution Unlimited

11. SUPPLEMENTARY NOTES	12. SPONSORING MILITARY ACTIVITY
	Naval Ship Systems Command Washington, D.C. 20362

13. ABSTRACT

A rotating disk apparatus, designed to attain high shear stresses comparable to those about hulls of full-scale ships is evaluated. It was thought that this apparatus could provide a convenient and inexpensive method to study frictional resistance of a full-scale ship. For a full-scale ship Reynolds number of 10^9, the average shear coefficient is approximately 0.0015. To attain the shear stress associated with such a shear coefficient, the angular velocity for a 2-ft diam disk is required to be about 350 rpm in water or about 10,000 rpm in air. These angular velocities were not obtainable with the disk apparatus described. However, the investigation did provide worthwhile results for lower shear stress values. Shear stresses were not measured but were inferred from measurements of disk moments. Two disk surfaces are evaluated, hydraulically smooth and sandpaper rough. For the smooth and rough surface disks in air, the experimental moment coefficients are generally greater than the theoretical predictions. Only the smooth surface disk was evaluated in water with results lower than predictions. The maximum Reynolds numbers attained in air and in water were 1.34×10^6 and 1.55×10^6, respectively.

Unclassified
Security Classification

Unclassified
Security Classification

14. KEY WORDS	LINK A		LINK B		LINK C	
	ROLE	WT	ROLE	WT	ROLE	WT
Frictional Resistance						
Rotating Disk						
Moment Coefficient						
Viscous Fluid						

DD FORM 1 NOV 65 1473 (BACK)
(PAGE 2)

Unclassified
Security Classification